orthorhombic and cubic Sb_2O_3. If the volume of the Sb^{III} cation together with its lone pair is computed like that of an oxygen atom, these figures lower to 15.4 and 15.2 Å^3 for Sb_2O_4 and 16.6 and 17.3 Å^3 for the two forms of Sb_2O_3. This indicates that the oxygen packing in α- and β-Sb_2O_4 is more dense than in the case of orthorhombic and cubic Sb_2O_3.

As indicated in Figure 4, the coordination of trivalent Sb2 in both forms of Sb_2O_4 can also be considered as very distorted octahedral (δ = 1613 and 1150, for α and β forms, respectively), if two more oxygen atoms at relatively larger distances are taken into account. When only the four shortest Sb2-O distances of Table III (between 2.019 and 2.238 Å for α-Sb_2O_4 and between 2.018 and 2.221 Å for the β form) are considered, the sums of the bond valences of Sb(III) equal 2.58 and 2.55, rather low values for trivalent Sb of α- and β-Sb_2O_4, respectively. However, taking into account two additional bonds (2.584 and 2.913 Å for the α form and two bonds of 2.932 Å for β-Sb_2O_4) the sums of the bond valences for both Sb(III) atoms become close to 3, 2.95 for α-Sb_2O_4 and 2.87 in the case of β-Sb_2O_4. On the other hand, the sums of the bond valences[13] for pentavalent Sb1 are 4.96 and 4.91 for the α and β forms, respectively.

Acknowledgment. We acknowledge a fellowship to C.R.V. and the financial aid of the Consejo Superior de Investigaciones Cientificas.

Registry No. Sb_2O_4, 1332-81-6.

Supplementary Material Available: Listings of anisotropic thermal parameters for α-Sb_2O_4 and β-Sb_2O_4 (1 page); listings of observed and calculated structure factors for α-Sb_2O_4 and β-Sb_2O_4 (6 pages). Ordering information is given on any current masthead page.

(12) Gutiérrez Puebla, E.; Gutiérrez Rios, E.; Monge, A.; Rasines, I. *Acta Crystallogr., Sect. B: Struct. Crystallogr. Cryst. Chem.* **1982**, *B38*, 2021.
(13) Brown, I. D.; Wu, K. K. *Acta Crystallogr., Sect. B: Struct. Crystallogr. Cryst. Chem.* **1976**, *B32*, 1957.
(14) Fischer, R. X. *J. Appl. Crystallogr.* **1985**, *18*, 258.
(15) Johnson, C. K. "ORTEP, A Fortran thermal-ellipsoid plot program for crystal structure illustrations"; Report ORNL-3794; Oak Ridge National Laboratory: Oak Ridge, TN, 1965.

Contribution from the Department of Inorganic Chemistry, University of Umeå, S-901 87 Umeå, Sweden, and Department of Physical Chemistry, Ruder Bošković Institute, Bijenička 54, YU-41001 Zagreb, Yugoslavia

Equilibrium and Structural Studies of Silicon(IV) and Aluminum(III) in Aqueous Solution. 16. Complexation and Precipitation Reactions in the H^+-Al^{3+}-Phthalate System

T. Hedlund,[†] H. Bilinski,[‡] L. Horvath,[‡] N. Ingri,[†] and S. Sjöberg*[†]

Received September 23, 1987

Equilibria in the title system were studied in 0.6 mol dm^{-3} Na(Cl) medium (25 °C) by using potentiometric (glass electrode) and tyndallometric methods. The Al complexation is characterized by the formation of the binary species AlL^+ and AlL_2^- as well as by the polynuclear mixed hydroxo complexes $Al_3(OH)_4L^{3+}$, $Al_2(OH)_2L^{2+}$, and $Al_2(OH)_2L_2$. The mononuclear species are of intermediate stability ($\log \beta_1 = 2.94 \pm 0.02$, $\log \beta_2 = 4.97 \pm 0.14$), whereas the polynuclear complexes show a higher stability (cf. $\log k(Al_3(OH)_4^{5+} + L^{2-} \rightleftarrows Al_3(OH)_4L^{3+}) = 5.10 \pm 0.03$). A solid phase with the composition $Al_2(OH)_4L \cdot 4H_2O$ was found to determine the precipitation boundary. The following formation constant was deduced: $\log k(2Al^{3+} + L^{2-} + 4H_2O \rightleftarrows Al_2(OH)_4L(s) + 4H^+) = 8.44 \pm 0.08$. This phase may be considered as the first precipitation step in the hydrolysis of aqueous aluminum phthalates to stable aluminum hydroxide and aluminate ions. The solid phase has also been characterized from X-ray analysis of powders, TGA, and IR spectra. Considering the phthalate ion as a possible binding site in humic substances, the significance of complexation and precipitation reactions in natural waters are discussed.

Introduction

The present work forms part of a research program on complexation and precipitation reactions in aluminosilicate systems comprising different organic ligands. In preceding publications homogenous[1] and heterogenous[2] equilibria characterizing the subsystem H^+-Al^{3+}-oxalic acid were studied. By the combination of results from precise equilibrium-analytical solution data with precipitation boundary data, it became possible to determine the composition and stability of the solid phases formed. It was found that the formed precipitates could be considered as the first metastable phases in the hydrolytic transformation of the aqueous AlL_n complexes down to stable aluminum hydroxide. This transition could be written as a series of complexation-hydrolysis reactions according to the scheme

$$Al^{3+} \rightleftarrows AlL_n(aq) \rightleftarrows Al_q(OH)_pL_r(aq) \rightleftarrows Al_q(OH)_pL_r(s) \rightleftarrows Al(OH)_3(s) \rightleftarrows Al(OH)_4^-$$

Out of the two phases formed, $Al_3(OH)_7Ox \cdot 3H_2O$ (Ox = oxalate) was found to be a possible solid phase in oxalate-rich ($>10^{-4.9}$ mol dm^{-3}) natural waters. Furthermore, this phase was indicated to have an octahedrally ordered sheet structure where oxalate ions were chelated on the sheet surface functioning as a bridge between two Al atoms. The ligands in this layer may then be substituted by various other ligands, e.g. silicic acid or silicate ions. Such a Si substitution may be the first step in an initial clay formation.

The objective of the present study is to study complexation and precipitation reactions in another subsystem, viz. the H^+-Al^{3+}-phthalate (L^{2-})-Na^+ system. Phthalate (L^{2-}) was chosen as a simple ligand containing carboxylic groups with an aromatic ring, both characteristic of natural humic substances. To our knowledge a complete characterization of these reactions has not been presented before. According to Napoli and Liberti,[3] the Al speciation is given by the two species AlL^+ ($\log k_1 = 3.18$) and AlL_2^- ($\log k_2 = 3.14$). The measurements were performed at 25 °C in 0.5 M $NaClO_4$ with $-\log [H^+] \leq 3.5$, where the possible formation of mixed Al^{3+}-L^{2-}-OH^- complexes was neglected. As these types of species frequently are formed, especially close to the precipitation boundaries, a full understanding of precipitation reactions and mechanisms is not possible unless such species are taken into consideration.

[†] University of Umeå.
[‡] Ruder Bošković Institute.

(1) Sjöberg, S.; Öhman, L.-O. *J. Chem. Soc., Dalton Trans.* **1985**, 2665.
(2) Bilinski, H.; Horvath, L.; Ingri, N.; Sjöberg, S. *Geochim. Cosmochim. Acta* **1985**, *50*, 1911.
(3) Napoli, A.; Liberti, A. *Gazz. Chim. Ital.* **1970**, *100*, 906.

0020-1669/88/1327-1370$01.50/0

Materials and Methods

Chemicals and Analysis. Phthalic acid, $C_8H_6O_4$ (Merck p.a.), was used without further purification after drying. Stock solutions were prepared by dissolving the acid in water, and the ligand content was determined potentiometrically. The titrated amount was found to be 0.5% lower than that expected from weighing. The preparations of other solutions are fully described elsewhere.[4]

Apparatus. The automatic system for precise emf titrations has been described by Ginstrup.[5] A Zeiss tyndallometer in combination with a Pulfrich photometer was used to detect the formation of solid phases. X-ray powder diffractograms were taken with a Rigaku/"Geigerflex" D/MAX II A diffractometer, using Cu Kα radiation. IR spectra were recorded on a Perkin-Elmer infrared spectrophotometer, Model 580 B. Thermogravimetric analyses (TGA) were carried out on a Cahn RG electroanalytical balance with a heating rate of 2 °C/min in air.

Temperature and Medium. The present investigation was carried out at 25.0 ± 0.1 °C in a constant ionic strength medium of 0.6 M Na(Cl).

Potentiometric Measurements. The titration procedures, including a special procedure to calibrate the glass electrode, have been described in earlier papers.[4,6] The reproducibility and reversibility of equilibria were tested by performing both forward (increasing –log [H^+] coulometrically) and backward (decreasing –log [H^+] by means of H^+ additions) titrations.

The acidity constants of phthalic acid were determined in separate titrations.

The three-component titrations were performed at a constant ratio of the total concentration of aluminum, B, and phthalate, C. The upper –log [H^+] limits in these titrations were set by the formation of precipitates.

Tyndallometric Measurements. The precipitation boundary was determined by using a tyndallometric technique as first described by Tezak et al.[7] and recently further discussed by Bilinski et al.[2] All solutions were equilibrated at 298 K for 24 h before the turbidity and pH were measured. The clear point was defined as a point showing the turbidity value of bidistilled water. The first turbid point was defined as a point with a weak Tyndall effect as close as possible to the last clear point.

Preparation of Solid Phases and Chemical Analyses. A number of precipitates were isolated from solutions close to the precipitation boundary at various total concentrations of aluminum and various molar ratios of total phthalate (C) and total aluminum (B). The aging time was 24 h. Samples were filtered through a Millipore filter (0.45 μm), washed with water, and dried in a desiccator with silica gel. Some samples were washed with 95% ethanol to remove excess NaCl prior to sodium and X-ray analysis. Plastic bottles were used instead of glassware for preparation of the solid phase, to prevent possible contamination with silicate.

The densities of the crystalline precipitates were determined by picnometry using paraffin oil.

The solid phase of the present study was chemically analyzed as described earlier.[2]

Data Treatment. The equilibria that must be considered in the present study can be divided into groups as

(i) protonation of phthalate

$$L^{2-} + nH^+ \rightleftarrows H_nL^{n-2},\ n = 1, 2 \quad \beta_{1,0,1} \text{ and } \beta_{2,0,1} \tag{1}$$

(ii) hydrolysis of Al^{3+}

$$pH^+ + qAl^{3+} \rightleftarrows H_pAl_q^{p+3q} \quad \beta_{p,q,0} \tag{2}$$

(iii) three-component equilibria of the general form

$$pH^+ + qAl^{3+} + rL^{2-} \rightleftarrows H_pAl_qL_r^{p+3q-2r} \quad \beta_{p,q,r} \tag{3}$$

Regarding eq 1, we will make use of results obtained in separate potentiometric titration experiments. For the hydrolytic equilibria of Al^{3+} (i.e. eq 2) we will use the results obtained in earlier papers[8,9] of this series, showing the occurrence of $AlOH^{2+}$ (log $\beta_{-1,1,0} = -5.52$), $Al_3(OH)_4^{5+}$ (log $\beta_{-4,3,0} = -13.57$), $Al_{13}O_4(OH)_{24}^{7+}$ (log $\beta_{-32,13,0} = -109.2$), and $Al(OH)_4^-$ (log $\beta_{4,1,0} = -23.46$).

In the evaluation of three-component data, these binary complex models were considered as known and all effects above this level treated as being caused by three-component species. The mathematical analysis of data was performed with the least-squares computer program LETAGROPVRID[10] (version ETITR[11]). pqr triplets and corresponding equilibrium constants that "best" fit the experimental data were determined by minimizing the error squares sum $U = \sum(H_{calcd} - H_{exptl})^2$ or $U = \sum(Z_{calcd} - Z_{exptl})^2$. H is defined as the total proton concentration calculated over the 0 level H_2O, Al^{3+}, L^{2-}. Furthermore, Z is defined as the average number of protons bound per L^{2-}, i.e. $Z = (H - [H^+] + k_w[H^+]^{-1})/C$.

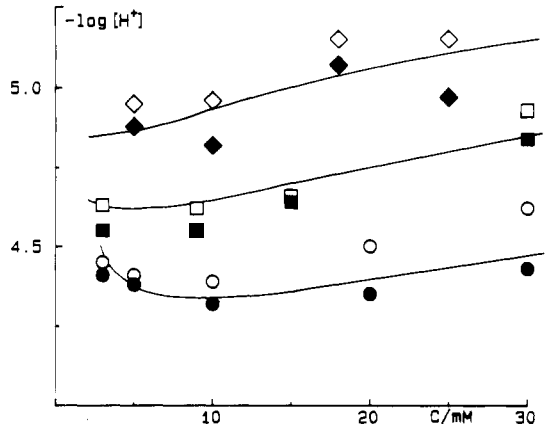

Figure 1. Selected data for tyndallometric measurements at different C/B ratios: (circles) B = 10 mmol dm^{-3}; (squares) B = 3 mmol dm^{-3}; (diamonds) B = 1 mmol dm^{-3}. Unfilled and filled symbols denote the –log [H^+] value where the first observation of precipitation occurred and that for the last clear point, respectively. The curves drawn represent the calculated precipitation boundaries for $Al_2(OH)_4L(s)$ (log $K_s = -8.44$).

Table I. X-ray Powder Diffraction Data of the Phase $Al_2(OH)_4L{\cdot}4H_2O$

2θ, deg	d_{obsd}, Å	d_{calcd}, Å	h	k	l	I/I_0
6.793	13.004	12.925	0	2	0	8
8.492	10.408	10.382	2	0	0	100
15.445	5.729	5.730	0	0	1	46
16.445	5.379	5.368	1	1	1	16
17.125	5.174	5.170	0	5	0	11
18.179	4.877	4.874	2	1	1	10
18.606	4.767	4.772	0	3	1	6
20.139	4.406	4.406	–3	1	1	41
21.507	4.128	4.130	3	2	1	8
25.950	3.430	3.430	6	1	0	18
27.395	3.253	3.253	2	6	1	10

Experimental Data

Potentiometric Data. Five titrations (163 experimental points) were performed in order to determine binary H^+–L^{2-} equilibria. The studied concentration ranges were $0.002 \le C \le 0.016$ mol dm^{-3} and $2.0 \le$ –log [H^+] ≤ 6.3. The following equilibrium constants were obtained: log $\beta_{1,0,1} = 4.652 \pm 0.003$ (3σ) and log $\beta_{2,0,1} = 7.281 \pm 0.004$ with a resulting $\sigma(Z) = 0.003$. These protonation constants are in good agreement with data in the literature.[14] Al complexation was studied within the ranges (27 titrations, 579 points) $0.001 \le B \le 0.010$, $0.001 \le C \le 0.016$ mol dm^{-3}, and $2.1 \le$ –log [H^+] ≤ 4.9. The following ratios C/B were investigated: 1/5, 1/3, 1/2, 1, 2, 4, 6, 8, and 16.

Precipitation Data. Experimental data for the precipitation boundary were collected for B = 1, 2, 3, 5 and 10 mmol dm^{-3}, with C/B ratios ranging from 1/3 to 25. Some of these experimental data are displayed in Figure 1.

Chemical analysis has shown that two phases determine the solubility boundary: amorphous $Al(OH)_3$ and $Al_2(OH)_4L{\cdot}4H_2O$ (L = phthalate). The second phase was further characterized. It has been obtained close to the precipitation boundary at room temperature from solutions at $1 \le C/B \le 25$. (Anal. Found: Al, 15.2; C, 26.3; H, 4.6. Calcd: Al, 15.1; C, 26.8; H, 4.5.) It was prepared in a microcrystalline form at B = 10 mmol dm^{-3} and C/B = 1 and was found to give a rather good X-ray

(4) Öhman, L.-O.; Sjöberg, S. *Acta Chem. Scand., Ser. A* **1981**, *A35*, 201.
(5) Ginstrup, O. *Chem. Instrum. (N.Y.)* **1973**, *4*, 141.
(6) Sjöberg, S. *Acta Chem. Scand.* **1971**, *25*, 2149.
(7) Tezak, B.; Matijevic, E.; Schultz, B. *J. Am. Chem. Soc.* **1951**, *73*, 1602.
(8) Öhman, L.-O.; Forsling, W. *Acta Chem. Scand., Ser. A* **1981**, *A35*, 795.
(9) Öhman, L.-O.; Sjöberg, S.; Ingri, N. *Acta Chem. Scand., Ser. A* **1983**, *A37*, 561.
(10) Ingri, N.; Sillén, L. G. *Ark. Kemi* **1964**, *23*, 97.
(11) Arnek, R.; Sillén, L. G.; Wahlberg, O. *Ark. Kemi* **1969**, *31*, 353. Brauner, P.; Sillén, L. G.; Whiteker, R. *Ark. Kemi* **1969**, *31*, 365.
(12) Eriksson, G. *Anal. Chim. Acta* **1979**, *112*, 375.
(13) Dyrssen, D.; Ingri, N.; Sillén, L. G. *Acta Chem. Scand.* **1961**, *15*, 694.
(14) Perrin, D. D. *Stability Constants of Metal-ion Complexes*; Pergamon: Oxford, England, 1979; Part B (Organic Ligands).

Table II. Result of LETAGROP Calculations for Different Assumptions Concerning Mixed Al^{3+}–L^{2-}–OH^- Complexes Formed[a]

Calculation of Different Models								
pairs of complexes tested	log ($\beta_{p,q,r} \pm 3\sigma$)	U	pairs of complexes tested	log ($\beta_{p,q,r} \pm 3\sigma$)	U	pairs of complexes tested	log ($\beta_{p,q,r} \pm 3\sigma$)	U
(−2,2,1)	−2.38 ± 0.05	12.7	(−3,3,2)	−1.37 ± 0.18	18.4	(−4,4,2)	−2.29 ± 0.14	12.9
(−4,2,1)	−11.45 ± 0.13		(−2,2,1)	−2.36 ± 0.04		(−3,2,1)	−6.97 ± 0.15	
(−2,2,1)	−2.62 ± 0.05	3.7	(−3,3,2)	−1.25 ± 0.15	6.8	(−4,4,2)	−2.31 ± 0.09	7.5
(−4,3,1)	−8.45 ± 0.05		(−3,3,1)	−3.99 ± 0.05		(−4,3,1)	−8.45 ± 0.08	
(−2,2,1)	−2.47 ± 0.03	4.2	(−3,3,2)	−1.00 ± 0.09	6.3	(−4,4,2)	−2.13 ± 0.05	7.3
(−6,4,1)	−14.52 ± 0.07		(−4,4,1)	−5.64 ± 0.07		(−6,4,1)	−14.57 ± 0.10	

Final Calculation with Proposed Model (U = 2.1)

species	(0,1,1)	(0,1,2)	(−2,2,1)	(−4,3,1)	(−2,2,2)
log $\beta \pm 3\sigma$	2.94 ± 0.02	4.97 ± 0.14	−2.50 ± 0.02	−8.47 ± 0.03	−0.07 ± 0.06

[a] The formation constants are defined according to the relation $pH^+ + qAl^{3+} + rL^{2-} \rightleftarrows H_pAl_qL_r^{p+3q-2r}$

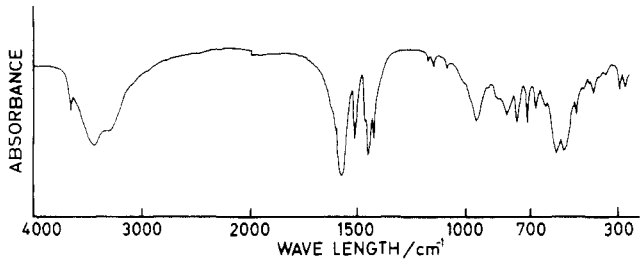

Figure 2. IR spectrum of $Al_2(OH)_4L{\cdot}4H_2O$ precipitated at B = 10 mmol dm^{-3}, C = 10 mmol dm^{-3}, −log [H^+] = 4.54, and 0.6 M NaCl.

powder diffractogram. The peaks could be indexed with a monoclinic unit cell of the dimensions a = 20.17 Å, b = 25.85 Å, c = 5.73 Å, and β = 91.45°. The data are presented in Table I in the form of 2θ, corresponding d_{obsd} and d_{calcd} spacings, and relative intensities for the 11 highest peaks. With the molecular weight M_r = 357.94 and molecular volume V = 3077.7 Å^3 the crystal density is given by the expression D_{calcd} = 0.193Z, where Z is the number of formula units in the unit cell. The experimentally determined density D_{measd} = 1.59 in paraffin oil can be satisfactorily explained if we assume Z = 8 (D_{calcd} = 1.55). As the number of lines is limited and single crystals have not been obtained, structural parameters can be considered as tentative.

From thermogravimetric analysis one can observe that the decomposition temperature is 299 K. The weight decreased slowly upon heating without a pronounced plateau up to 678 K. Above this temperature rapid decomposition occurs. The total weight loss up to 973 K was 69.6%. The degradation product was identified by X-ray diffraction as ι-alumina (Al_2O_3),[15] containing also some unidentified peaks of smaller intensity (at d = 4.10, 3.94, 3.85, 3.62, 2.80, 2.53, 2.28, 2.11, 1.96, 1.87, 1.72, 1.64, 1.61 Å).

Infrared Study. The infrared spectrum of $Al_2(OH)_4L{\cdot}4H_2O$ is given in Figure 2. Only the most characteristic features of the IR spectra will be discussed, with use of the conventions of Nakamoto.[16] The compound shows a broad absorption band in the region 3000–3750 cm^{-1}, which originates from O–H stretchings of water molecules and OH^- groups. The broadness of this absorption band indicates the presence of hydrogen bonding. The main absorption band at 1690 cm^{-1} in phthalic acid is shifted to 1570 cm^{-1} in the salt (asymmetric stretching frequency of coordinated COO^- groups). The strong band at 1400 cm^{-1} in phthalic acid due to symmetric stretching of the carboxyl group and the strong and broad band at 1280 cm^{-1} due to in-plane OH^- deformation are both shifted to higher frequencies, giving a composite band with peaks at 1450 and 1430 cm^{-1}. The OH^- deformation vibration of the carboxyl group found at 910 cm^{-1} in phthalic acid does not exist in the aluminum phthalate. It seems to be shifted to 950 cm^{-1}. The broad band with resolved peaks at 580 and 540 cm^{-1} is possibly due to Al–OH stretches. The small separation of the composite ν_a and ν_s frequencies suggests that phthalate ion acts as a bidentate ligand bound to one aluminum atom.

Calculations and Results

Homogeneous Equilibria. The equilibrium analysis was started by plotting $\bar{n}$ vs −log[L^{2-}] and Z vs −log [H^+] curves. (cf. Figures 3 and 4, respectively.) Coinciding $\bar{n}$ curves are found if predominating mononuclear AlL_n complexes are formed. According to Figure 3 an approximate limiting curve with $\bar{n} < 0.5$ and $C/B \geq 8$ is found. These data were used to calculate approximate formation constants for AlL and AlL_2 (log $\beta_{0,1,1}$ = 2.89 ± 0.04 and log $\beta_{0,1,2}$ = 4.97 ± 0.10).

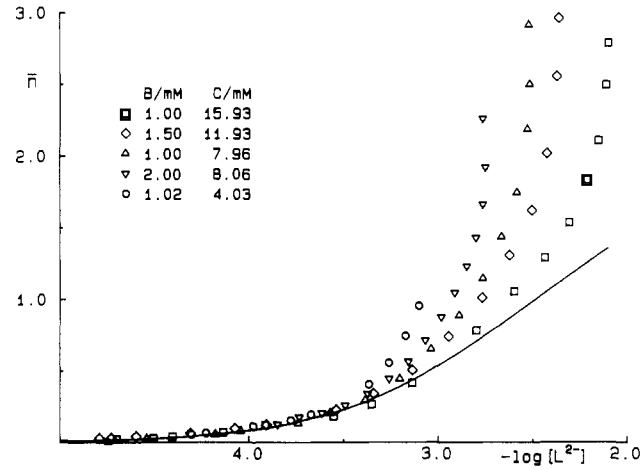

Figure 3. Experimental data plotted as $\bar{n}$ vs −log [L^{2-}] curves for C/B ratios 4, 8, and 16. The curve drawn has been calculated with the binary complexes AlL^- and AlL_2 (log $\beta_{0,1,1}$ = 2.94 and log $\beta_{0,1,2}$ = 4.27).

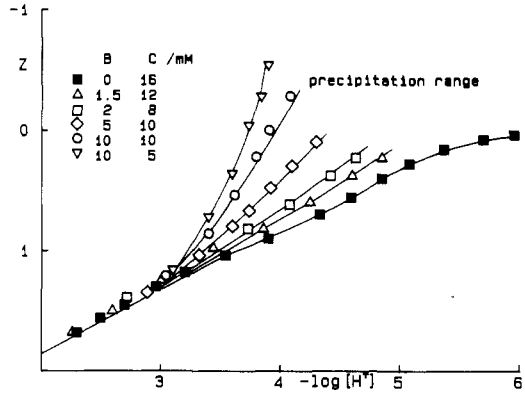

Figure 4. Experimental data plotted as curves Z vs log [H^+] curves. The curves drawn have been calculated with the set of proposed constants.

Deviations from the "mononuclear" curve indicate the formation of mixed $Al_q(OH)_pL_r$ complexes. A systematic testing of different p,q,r combinations from data with $C/B \geq 4$ showed the species $Al_2(OH)_2L_2$ to give the "best" fit to experimental data (cf. Figure 5). Attempts were also made to evaluate the stability of a possible AlL_3^{3-} complex. These failed, however, showing this complex to be formed in negligible amounts within the concentration ranges studied.

With $1/5 \leq C/B \leq 2$, the formation of mixed Al^{3+}–L^{2-}–OH^- complexes is even more pronounced. This can be seen from Figure

(15) Foster, J. *Electrochem. Soc.* **1959**, *106*, 971. (Powder Diffraction File 12-539).
(16) Nakamoto, K. *Infrared and Raman Spectra of Inorganic and Coordination Compounds*, 3rd ed.; Wiley: New York, 1978.

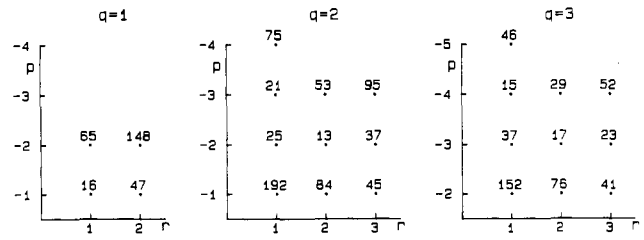

Figure 5. Results of p,q,r analysis on data with $C/B > 4$. The figures give the error squares sum $U_H(pr)_q$, assuming one new ternary complex.

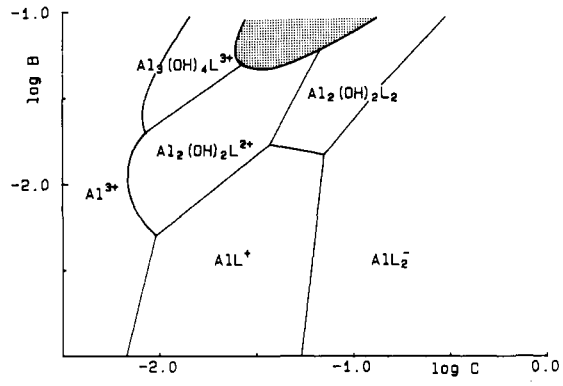

Figure 6. Predominance area diagram at $-\log [H^+] = 4$. The shaded region represents the precipitation area of $Al_2(OH)_4L(s)$.

4, where $Z < 0$ is a direct proof of their formation. Another systematic search was performed ($1 \leq C/B \leq 4$), which clearly showed these complexes to be polynuclear. The "best" candidates turned out to be species with $-p = q$ and $q > r$, viz. (−2,2,1), (−3,3,2), and (−4,4,2). However, none of these species could satisfactorily explain the experimental data. Furthermore, it was found that additional species are formed at the lowest ratios studied ($C/B = 1/5, 1/3, 1/2$). From data with $1/5 \leq C/B \leq 4$, speciation schemes were tested, where, besides one of the candidates given above, one additional complex was introduced. In total 60 combinations were tested, and those giving the lowest error squares sums are given in Table II. As can be seen, the best fit was obtained by assuming the complexes $Al_3(OH)_4L^{3+}$ and $Al_2(OH)_2L^{2+}$ to be formed. These two are also likely for structural reasons.

In a final calculation the formation constants of the different species were refined, with the results presented in Table II.

Attempts were also made to introduce the mononuclear species Al(OH)L and $Al(OH)L_2^{2-}$. However, no significant improvement of the fit to experimental data was obtained.

In order to visualize the speciation in the present system, a predominance area diagram valid at $-\log [H^+] = 4$ was constructed (cf. Figure 6). As seen, AlL^+ and AlL_2^- both predominate at low B ($B \lesssim 10^{-2.2}$ mol dm^{-3}). At higher B, the formation of the mixed hydroxo complexes becomes extensive. Additional calculations show that, with increasing $-\log [H^+]$ values, they predominate at still lower B, vis. $\sim 10^{-4}$ and $\sim 10^{-5}$ mol dm^{-3} with $-\log [H^+] = 5$ and 6, respectively.

Heterogeneous Equilibria. By knowing the speciation in solution, it has become possible to determine a formation constant for the solid phase $Al_2(OH)_4L \cdot 4H_2O$. This constant ($\beta_{-4,2,1}$) is defined according to the equilibrium

$$2Al^{3+} + 4H_2O + L^{2-} \rightleftarrows Al_2(OH)_4L(s) + 4H^+$$

In the calculations the average value of $-\log [H^+]$ in the last clear point and first turbid point was used as a "precipitation point". Furthermore, the amount of precipitate at these points was assumed to be negligible. This implies that a calculation of $\beta_{-4,2,1} = [H^+]^4[Al^{3+}]^{-2}[L^{2-}]^{-1}$ at each precipitation point is possible by using experimental $-\log [H^+]$, B, C data. The results showed that a constant value in $\beta_{-4,2,1}$ was obtained, provided $C/B \geq 1/2$.

At the lowest ratios studied ($C/B = 1/3, 1/5$) the calculations showed that significant amounts of $Al_{13}O_4(OH)_{24}^{7+}$ are formed. However, this complex is known to form very slowly at room temperature.[8,17] The present solubility data represent measurements made after 24 h, which is too short a time for this complex to equilibrate. However, setting the amount of (−32,13,0) to 0 eliminated the drift of $\beta_{-4,2,1}$, analogous to the situation observed for the aluminum oxalate system.[2]

When the error squares sum $U = \sum(\log [H^+]_{calcd} - \log [H^+]_{expti})^2$ was minimized, the refined value $\log \beta_{-4,2,1} = -8.44 \pm 0.08$ (3σ) with $\sigma(-\log [H^+]) = 0.08$ was obtained.

Discussion

Speciation and Equilibria. Al complexation in the present system is characterized by the formation of binary AlL_n^{3-2n} species ($n = 1, 2$) as well as the polynuclear mixed hydroxo complexes $Al_3(OH)_4L^{3+}$, $Al_2(OH)_2L^{2+}$, and $Al_2(OH)_2L_2$.

The values of the stepwise constants ($\log k_1 = 2.94$ and $\log k_2 = 2.03$) show AlL^+ and AlL_2^- to be of intermediate stability. A comparison with values given by Napoli and Liberti[3] shows a fair agreement in $\log k_1$. On the other hand, they found AlL_2^- to be of the same stability as AlL^+ ($\log k_1 \approx \log k_2$). This high stability in AlL_2^- is somewhat unexpected, especially in Al systems with charged ligands where electrostatic effects are significant. In view of the present results, a plausible explanation for this "stabilization" is that Napoli and Liberti[3] neglected the formation of mixed hydroxo species.

A comparison with oxalate[1] as ligand clearly shows that the different oxalate AlL_n^{3-2n} species are stronger ($\log k_1 = 6.03$, $\log k_2 = 4.90$, and $\log k_3 = 3.99$) than the corresponding phthalate species. This difference is attributed to the high stability of five-membered chelate rings (oxalate) compared to that of seven-membered rings (phthalate). However, it can be noted that the electrostatic effects reflected in the ratios $\log (k_{n+1}/k_n)$ are the same magnitude irrespective of the ligands.

A comparison between AlL_n complexes with the ligand being phthalate (Ph), salicylate (S), and pyrocatechol (Py) clearly shows the stability of these species to increase within the series Ph (2.94, 2.03, –) < S[18] (12.77, 10.48, –) < Py[19] (15.86, 13.10, 9.02). Values in parentheses denote the corresponding stepwise constants ($\log k_n$).

According to the predominance area diagram given in Figure 6, the formation of di- and trinuclear mixed hydroxo complexes is extensive, close to the precipitation boundary. This was also found in the corresponding oxalate system,[1] where the species $Al_3(OH)_3L_3$ and $Al_2(OH)_2L_4^{4-}$ were formed. The high stability of these polynuclear complexes can be demonstrated by calculating constants defined according to the equilibria

$$Al_3(OH)_4^{5+} + L^{2-} \rightleftarrows Al_3(OH)_4L^{3+} \quad \beta_{1,3}$$

$$Al_2(OH)_2^{4+} + nL^{2-} \rightleftarrows Al_2(OH)_2L_n^{4-2n} \quad \beta_{n,2}$$

In the phthalate system $\log \beta_{1,3} = 5.10$, $\log \beta_{1,2} \gtrsim 5.5$, and $\log \beta_{2,2} \gtrsim 8$. Though the existence of the dimer $Al_2(OH)_2^{4+}$ has been questioned,[8,20] a value of $\log \beta_{-2,2,0} \leq -8$ was used in these recalculations. This implies that the $Al_3(OH)_4^{5+}$ (and $Al_2(OH)_2^{4+}$) complex forms stronger complexes with phthalate than the Al^{3+} ion. Similar results have been found in the gallic acid[21] ($\log \beta_{1,3} = 5.20$) and oxalic acid[1] systems ($\log \beta_{4,2} = 21.54$).

Solubilities and Phase Relations. The solubility boundary was found to be determined by the solid-phases $Al_2(OH)_4L \cdot 4H_2O$ and $Al(OH)_3$. A diagram showing the solubility and phase relations for $B = 10$ mM is given in Figure 7. This diagram clearly shows that a full description of the solubility characteristics of the present system is not possible unless the formation of mixed hydroxo complexes is taken into consideration.

(17) Aveston, J. *J. Chem. Soc.* **1965**, 4438.
(18) Öhman, L.-O.; Sjöberg, S. *Acta Chem. Scand., Ser. A* **1983**, *A37*, 875.
(19) Öhman, L.-O.; Sjöberg, S. *Polyhedron* **1983**, *2*, 1329.
(20) Brown, P. L.; Sylva, R. N.; Batley, G.; Ellies, J. *J. Chem. Soc., Dalton Trans.* **1985**, 1967.
(21) Öhman, L.-O.; Sjöberg, S. *Acta Chem. Scand., Ser. A* **1982**, *A36*, 47.

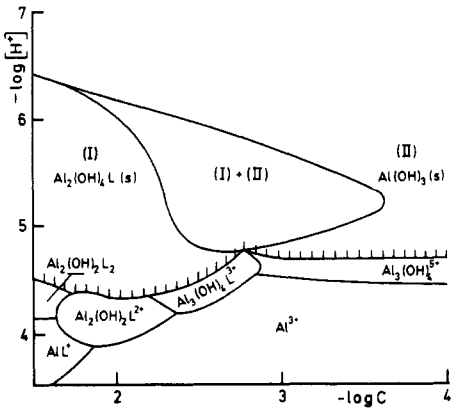

Figure 7. Predominance area diagram of $-\log [H^+]$ vs $(-\log C)_B$ for B = 10 mmol dm^{-3}. The diagram shows the predominating Al species as well as the stable ranges of solid phases.

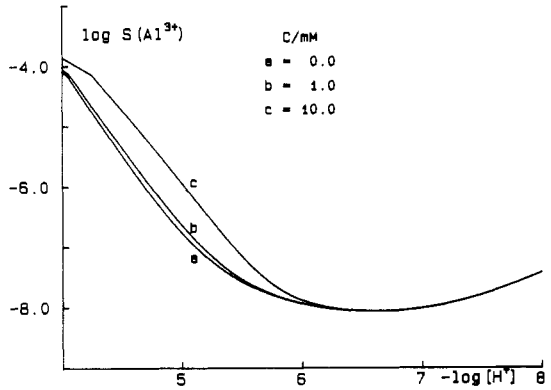

Figure 8. Solubility of kaolinite ($Al_2(OH)_4Si_2O_5$) (with respect to Al) in the presence of phthalate at different concentrations. The formation constant for kaolinite is according to Helgeson.[23]

The phthalate phase can be regarded as a hydrolysis product of the complexes $Al_2(OH)_2L^{2+}$ and $Al_2(OH)_2L_2$:

$$Al_2(OH)_2L^{2+} + 2H_2O \rightleftarrows Al_2(OH)_4L(s) + 2H^+$$

$$Al_2(OH)_2L_2 + 2H_2O \rightleftarrows Al_2(OH)_4L(s) + L^{2-} + 2H^+$$

On further hydrolysis this solid phase is transformed to aluminum hydroxide and $Al(OH)_4^-$ ions.

Modeling Calculations. It has been shown earlier that pyrocatechol[19] and salicylic acid[18] both enhance the dissolution of the clay mineral kaolinite ($Al_2(OH)_4Si_2O_5$). With pyrocatechol this influence was found in slightly alkaline solutions, whereas in the presence of salicylic acid the main influence was found at $-\log [H^+] \approx 5$. In the present work a similar model calculation was performed with phthalate. However, due to the weak Al complexation the dissolution of kaolinite in the presence of phthalate was less extensive (cf. Figure 8) than in the case of pyrocatechol and salicylic acid. A similar effect was observed on dissolution of δ-Al_2O_3 in the presence of salicylate, phthalate, and benzoate by Furrer and Stumm.[22]

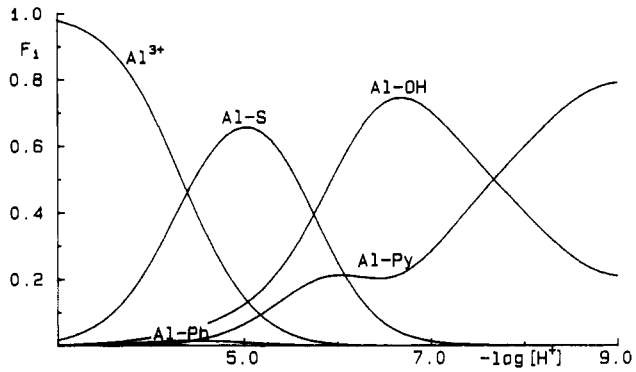

Figure 9. Distribution diagram of F_i vs $(-\log [H^+])_{BC}$ showing the sum of distribution coefficients, F_i, for aluminum phthalates (Al-Ph), aluminum salicylates (Al-S), aluminum pyrocatecholates (Al-Py), and aluminum hydroxides (Al-OH) as well as $F_{Al^{3+}}$. The total concentration of each ligand is equal to 0.1 mmol dm^{-3}. Kaolinite is the stable solid phase.

When these three aromatic bidentate ligands are regarded as possible binding sites in natural organic material, Figure 9 shows the complexation features of these sites to be quite different. *O*-dicarboxylic and *O*-carboxylic phenolic compounds are active in slightly acidic solutions, while *O*-diphenolic compounds are much more active in neutral and slightly alkaline solutions. As seen, the relative importance of aluminum bound to phthalate is negligible unless high (unnatural) concentrations are considered. It must also be noted that pure Al hydrolysis is predominating the speciation at neutral pH.

Finally, it was concluded that the phthalate phase $Al_2(OH)_4L\cdot 4H_2O$ is too soluble to be a likely precipitate in the environment. This is different from findings in the corresponding oxalate system.[2]

Acknowledgment. We thank Dr. Lars-Olof Öhman for much valuable discussion. This work forms part of a program financially supported by the Swedish Natural Science Research Council, by the Self-Management Community of Interest for Scientific Research of SR Croatia, and by the International Atomic Energy Agency, Vienna (Research Contract No. 3896/RI/RB).

Registry No. Al, 7429-90-5; $C_8H_6O_4$, 88-99-3; $Al_2(OH)_4L\cdot 4H_2O$, 112816-48-5.

(22) Furrer, G.; Stumm, W. *Geochim. Cosmochim. Acta* **1969**, *50*, 1847.
(23) Helgeson, H. C. *Am. J. Sci.* **1966**, *266*, 729.

Contribution from the Department of Chemistry, University of Idaho, Moscow, Idaho 83843

Preparation and Characterization of Chlorodifluorosulfur(IV) Hexafluoroarsenate

Kohrshed Alam and Jean'ne M. Shreeve*

Received September 23, 1987

The stable salt $[SF_2Cl]^+[AsF_6]^-$ was prepared and isolated in good yield from the reaction of *trans*-CF_3SF_4Cl and AsF_5. The identity and ionic nature of this salt were established by its elemental analysis and by ^{19}F NMR, IR, and mass spectral studies. Redistribution of the halogen atoms in the cation of $[SF_2Cl]^+[AsF_6]^-$ to form $[SF_3]^+[AsF_6]^-$ and $[SCl_3]^+[AsF_6]^-$ in liquid SO_2 occurred at ambient temperature. In the presence of NaF or NaCl, $[SF_2Cl]^+$ was converted to $[SF_3Cl]$ or $[SF_2Cl_2]$, respectively, at low temperature, where redistribution occurred to form SF_4 and $[SCl_4]$.

Salts that contain the $[SF_3]^+$ cation are formed readily by fluoride ion transfer reactions between sulfur tetrafluoride (SF_4) and fluorine-containing Lewis acids.[1,2] The lack of an appropriate precursor, e.g., SF_3Cl, has precluded the formation of $[SF_2Cl]^+$

0020-1669/88/1327-1374$01.50/0